Structural and Electronic Rearrangements upon the Oxidation of Binuclear (Ru 2) and Trinuclear (MoRu 2) Complexes with Bridging o- Phenylenediamido Ligands †

ARTICLE *in* ORGANOMETALLICS · FEBRUARY 2004

Impact Factor: 4.13 · DOI: 10.1021/om034223k

Available online at www.sciencedirect.com
SCIENCE DIRECT®
Inorganica Chimica Acta 350 (2003) 557–567
Inorganica Chimica Acta
www.elsevier.com/locate/ica

Structural and electronic features of Group 8 metal complexes containing one α-diiminobenzene chelate ligand

Adela Anillo [a], Santiago Garcia-Granda [b], Ricardo Obeso-Rosete [a,*], Agustín Galindo [c], Andrea Ienco [d], Carlo Mealli [d,*]

[a] *Departamento de Química Orgánica e Inorgánica, Instituto Universitario de Química Organometálica 'Enrique Moles', Julián Clavería s/n, 33071 Oviedo, Spain*
[b] *Departamento de Química Física y Analítica, Facultad de Química, Universidad de Oviedo, Julián Clavería s/n, 33071 Oviedo, Spain*
[c] *Departamento de Química Inorgánica, Universidad de Sevilla, Aptdo 553, 41071 Seville, Spain*
[d] *ICCOM, CNR, Via Nardi 39, 50132 Firenze, Italy*

Received 6 August 2002; accepted 4 October 2002

Article submitted in honour of Professor Pierre Braunstein

Abstract

Known complexes of general formula $L_nM(diim)$, where $diim = C_6H_4(NH)_2$-*o*, α-diiminobenzene, $n = 3$, 4 and M is a metal of Group 8 (Ru(II), in particular) are analyzed in terms of their electronic structure and associated energetics. The newly synthesized compound $[(CO)_2(PPh_3)BrRu(C_6H_4(NH)_2$-*o*$)]Br$, **1**, is a new member of the category. This is confirmed by the X-ray structure of **1** that is presented together with electrochemical measurements and other spectroscopic characterization. At variance with the isoelectronic L_4M(*o*-phenylenediamido) compounds (M = Group 6 metal) that are affected by structural deformations, **1** and similar complexes have a regular pseudo-octahedral structure. Density functional theory calculations and qualitative MO arguments provide an explanation for the different electronic trends as well as for the diimino/diamido dichotomy of the *non-innocent* chelate ligand. The latter is affected, not only by the nature of the metal (energy of d orbitals), but also by the surrounding environment (three or four coligands). Moreover, the calculations allow to outline the stability trends for the loss of one coligand from $L_4M(diim)$ systems when the Ru(II) complexes are chemically or electrochemically reduced.

Keywords: Diiminobenzene complexes; Group 8 metals; Density functional theory calculations; Theoretical analysis

1. Introduction

Transition metal complexes that contain at least one α-diiminobenzene chelate ($C_6H_4(NH)_2$-*o*, *diim*) are still the subject of many experimental and theoretical studies because of their effectiveness in homogenous catalysis [1]. Recently, their potentialities as DNA-binding intercalators have been tested [2]. This ligand may adopt a variety of coordination modes in mononuclear and polynuclear complexes and, in principle, it can be the donor of a different number of electron pairs (up to five in some binuclear species [3]). Interesting properties are due to the *non-innocence* of *diim* that may be stabilized in either the uncharged diimino or the dianionic diamido form (Scheme 1).

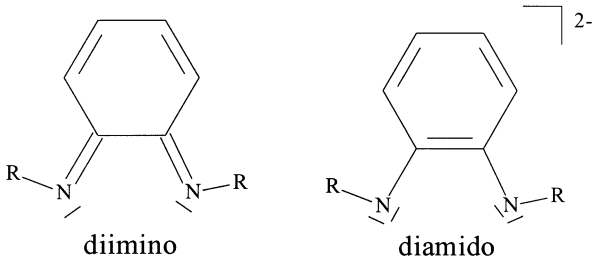

Scheme 1.

* Corresponding authors. Tel.: +39-55-234 6653; fax: +39-55-247 8366.
E-mail addresses: ror@sauron.quimica.uniovi.es (R. Obeso-Rosete), mealli@fi.cnr.it (C. Mealli).

0020-1693/03/$ - see front matter
doi:10.1016/S0020-1693(02)01557-8

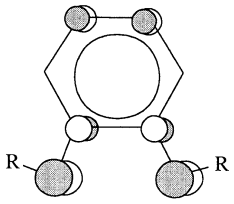

Scheme 2.

The electronic nature of the chelate can be discriminated, case by case, with experimental techniques (single crystal X-ray data, XPS, resonance Raman and others [4]), but also on the basis of theoretical calculations, better if supported by the simple concepts the perturbation theory. By considering the simplest mononuclear metal complexes, the diimino/diamido dichotomy may be shifted in one way or another by the nature of the metal and the environment of the coligands. This occurs because the chelate features a delocalized π* MO (Scheme 2) approximately in the energy region of the metal d orbitals. Ultimately, the relative order of ligand and metal energy levels will determine different photophysical, photochemical and electrochemical properties [5].

We report elsewhere [6] a detailed theoretical analysis (based on density functional theory (DFT) calculations and their qualitative interpretation) of selected $L_4M(o$-phenylenediamido) pseudo-octahedral complexes containing a metal of the Group 6 (Cr, Mo, W). Although limited, the latter series presents a variety of different electronic situations at the metal with the chelate invariably assuming the dianionic diamido status. In fact, whereas the metal oxidation number differs as much as VI, IV, II and possibly 0, the ligand's critical π* MO lies always below the variably occupied 't_{2g}' levels (Scheme 3). Accordingly, it must be considered fully occupied in all cases. In other words, the electron pair of the π^*/d_π bonding interaction (when the chelate lies in the equatorial plane) is assigned to the chelate irrespective of the metal d electron population (from d^0 to d^6).

In view of the π* nature of the chelate's HOMO (Scheme 2), the diamido formulation of the ligand implies single C–N bonds and a C=C double bond (right side of Scheme 1). Moreover, an accumulation of electron density occurs in the p_π orbitals of the nitrogen atoms. This is consistent with the generally long C–N distances (~ 1.4 Å) found in the series of Group 6 metal complexes [6]. Depending on the number of electrons

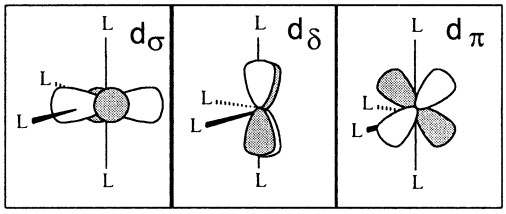

Scheme 3.

available to the Group 6 metal, the $L_4M[C_6H_4(NR)_2$-$o]$ complexes are subject to different types of distortion from the pseudo-octahedral geometry. For instance, in the d^0 species $Cl_2(NPh)(PMe_3)W[C_6H_4(NSiMe_3)_2$-$o]$ [7], the bending of the chelate off the equatorial plane allows the diamido chelate to use its filled π* level for donation into d_σ-orbital rather than in the d_π one. In fact, the latter already receives a strong donation from the axial imido ligand. Such a feature had been noted also for other d^0 diamido complexes with a number of coligands <4 [8]. For a d^4 complex such as $(CO)_2(PPh_3)_2Mo[C_6H_4(NH)_2$-$o]$ [9], Jahn–Teller effects [10] are responsible for rotation of the chelate about its C_2 axis, whereas for a d^2 configuration, the system may be stabilized in either a singlet (e.g., $(CO)(pyridine)_2(NPh)W[C_6H_4(NSiMe_3)_2$-$o]$ [11]) or a triplet ground state (e.g., $Cl_2(PMe_2Ph)_2Cr[C_6H_4(NH)_2$-$o]$ [12]). Finally, for a metal in the oxidation state 0 (d^6), complexes of formula $L_4M(o$-phenylenediamido) may be critically unstable to the loss of one coligand. For example, dianionic complexes with three CO coligands (e.g. $[(CO)_3W(o$-phenylenediamido)$]^{2-}$) have been synthesized and structurally characterized [13] but no example is reported of a diamido complex with four CO ligands. On the other hand, the latter type of complex are found with the comparable o-phenylenedisulfide or o-phenylenediphosphido chelates [14]. Ab initio calculations reported by Darensbourg et al. [14] and also those performed by some of us [6] indicate deeper energy stabilization for the pseudo-octahedral gas molecules. However, it should be stressed that, also in this case, competitive entropic factors can ultimately favor dissociation if the products are both stable molecules (namely, the five-coordinate W dianion and a free CO ligand).

We wish to extend now the theoretical considerations to the analogous $L_4M(diim)$ complexes of Group 8 metals. A search in the Cambridge databank [15] shows about 15 examples of the latter type of complexes and a single $L_3M(diim)$ derivative, namely the species $(PPh_3)_3Ru[C_6H_4(NH)_2$-$o]$, previously reported by some of us [16]. In several of the retrieved compounds the L_4M unit is formed by a polydentate ligand thus, for the sake of simplicity, we restrict our attention to the five species that carry four discrete coligands. These include a tetracyano Fe(II) complex [17] and four other Ru(II) complexes with mixed ligands such as PPh_3, acetonitrile, chloride and water [18]. To this series, we add newly synthesized halide complexes of formula $[(CO)_2(PPh_3)$-$XRu(diim)]X$ (X = Br, I, Cl). In particular, we will present in this paper the synthesis, electrochemistry and X-ray structure of the bromide derivative **1**. Moreover, the electronic structure of the complex cation in **1** and that of other relatable Ru(II) compounds of general formula $(PH_3)_nRu(diim)$ ($n = 3, 4$) has been explored by means of DFT calculations and qualitative MO theory.

The structural features and the energetic trends will be pointed out but, in particular, perturbation theory arguments will be used to highlight the interplay between the diimino/diamido nature of the chelate when bound to a Group 8 metal.

2. Experimental

2.1. General

All reactions and CV measurements were carried out under nitrogen. Solvents (except for PhCl that was used as supplied) were freshly distilled under nitrogen after drying with reflux over sodium (thf, hexane) or CaH_2 (CH_2Cl_2). Microanalytical data (C, H, and N) were obtained from a Perkin Elmer 240-B elemental analyzer. Infrared spectra were recorded from nujol mulls (KBr discs) or solutions (CaF_2 discs) with a Perkin Elmer 1720-XFT spectrometer. ^{31}P NMR spectra were recorded on a Bruker AC-300 spectrometer (data referenced to 85% external H_3PO_4). Electrochemical measurements were carried out with an Amel Electrochemolab instrument, used with a three-electrode cell. The working and auxiliary electrodes were of platinum while the reference was an aqueous saturated calomel electrode, separated from the solution by a porous frit and a KCl saturated agar bridge. A conductimeter CRISON micro CM 2201 was used.

The dinuclear and mononuclear compounds $(CO)_4(PPh_3)_2Ru_2[\mu\text{-}C_6H_4(NH)_2\text{-}o]$ and $(CO)_2(PPh_3)Ru[C_6H_4(NH)_2\text{-}o]$, that have been used as precursors of the presently synthesized compounds, were prepared according to the published procedures [16,19]. All others reagents were used as supplied without further purification.

2.1.1. Synthesis of the complex $[(CO)_2(PPh_3)BrRu(C_6H_4(NH)_2\text{-}o)]Br$, **1**

Compound $(CO)_4(PPh_3)_2Ru_2[\mu\text{-}C_6H_4(NH)_2\text{-}o]\cdot C_6H_5CH_3$ (0.60 g, 0.58 mmol) was dissolved in PhCl (8 ml) and an excess of Br_2 in PhCl (2 ml) was added dropwise while stirring. After 15 min. the red–orange crystalline solid was collected, washed with hexane and vacuum-dried (yield approximately 80% based on one of the two Ru of the starting compounds). Crystals suitable for X-ray diffraction analysis were obtained from a benzene–hexane solution. IR (nujol mull, cm^{-1}) 3103 w, 2080 vs, 2038 vs (2086 vs, 2040 s in CH_2Cl_2). Elemental analysis: C 49.49 (50.34)%, H 3.65 (3.56)%, N 3.50 (3.67) (in parentheses those expected for $\mathbf{1}\cdot C_6H_5Cl$). $^{31}P\{^1H\}$NMR: 43.75 ppm (s).

2.1.2. Synthesis of $[(CO)_2(PPh_3)IRu(C_6H_4(NH)_2\text{-}o)]I$

The procedure is the same as above but a I_2-PhCl solution was added. A dark brown crystalline solid was obtained (yield approximately 80%). IR (nujol mull, cm^{-1}) 3106 w, 2073 vs, 2033 vs (2073 vs, 2028 s in thf).

2.1.3. Synthesis of $[(CO)_2(PPh_3)ClRu(C_6H_4(NH)_2\text{-}o)]Cl$

The dinuclear complex $(CO)_4(PPh_3)_2Ru_2[\mu\text{-}C_6H_4(NH)_2\text{-}o]\cdot C_6H_5CH_3$ (0.30 g, 0.29 mmol) was dissolved in thf (5 ml) and the solution was stirred with an excess of $CuCl_2$ for 1 h. A brown-reddish crystalline residue was collected, washed with Et_2O and dried 'in vacuo' (yield $\approx$75%). IR (nujol mull, cm^{-1}) 2085 vs 2036 vs (2088 vs 2043 s in CH_2Cl_2).

2.1.4. General method to synthesize $[(CO)_2(PPh_3)XRu(C_6H_4(NH)_2\text{-}o)]X$ ($X = Cl, Br, I$)

The compound $(CO)_2(PPh_3)Ru[C_6H_4(NH)_2\text{-}o]$ (0.20 g, 0.32 mmol) and the proper halide (1 mmol) in a CH_2Cl_2 soluble form (e.g. PPNCl, LiBr or LiI) are stirred in CH_2Cl_2 (5 ml) with a slight excess of $[(Cp)_2Fe](PF_6)$ for 1 h. The solution is let to dry under vacuum and then washed with hexane. The complexes are recrystallized from CH_2Cl_2/hexane. Yields are over 90%.

2.2. Electrochemistry

Cyclic voltammetry of **1**, dissolved in CH_2Cl_2 (0.5×10^{-3} M) with $[(NBu^n_4)PF_6]$ as supporting electrolyte (0.1 mol l^{-1}), was performed at room temperature between 0 and -0.5 V at a scan rate of 50 mV s^{-1}. A reduction and an oxidation peak were observed at -0.20 and -0.08 V, respectively.

The conductivity of **1** (5×10^{-3} M in CH_3NO_2) was found to be 95 S cm^2 mol^{-1}.

2.3. X-ray experimental and crystal data for **1**

Crystal data and details of data collections are summarized in Table 1. A red crystal, with approximated dimensions of $0.17 \times 0.13 \times 0.13$ mm^3, was used for the measurements at 293(2) K.

The unit-cell parameters were determined from the angular settings of 25 reflections in the range $10 \leqslant \theta \leqslant 15^\circ$. The space group was inferred to be C_2/c from the systematic absences and confirmed by the successful determination of the structure. The intensities of 6444 reflections (after merging) were collected in the θ range 0–26° by using the $\omega-2\theta$ scan technique with a scan angle of 1.5° and a variable scan rate with a maximum scan time of 60 s per reflection. The Mo Kα radiation was used with a graphite–crystal monochromator on a Nonius CAD4 single-crystal diffractometer. The intensity

Table 1
Crystal data and structure refinement for $[(CO)_2(PPh_3)BrRu(C_6H_4(NH)_2\text{-}o)]Br\cdot C_6H_6$, **1**

Empirical formula	$C_{32}H_{27}Br_2N_2O_2PRu$
Formula weight	761.40
Temperature	293(2) K
Crystal system, space group	monoclinic, C_2/c
Unit cell dimensions	
a (Å)	25.495(6)
b (Å)	16.963(13)
c (Å)	15.263(6)
α (°)	90
β (°)	92.97(3)
γ (Å)	90
Volume (Å^3)	6592(6)
Z	8
D_{calc} (g cm^{-3})	1.534
Absorption coefficient (mm^{-1})	2.978
Wavelength (Å)	0.71073
$F(0\,0\,0)$	3008
Crystal size (mm)	$0.17 \times 0.13 \times 0.13$
θ range (°)	1.44–25.97
Limiting indices	$-31 \leqslant h \leqslant 31$, $0 \leqslant k \leqslant 20$, $0 \leqslant l \leqslant 18$
Reflections collected/unique	6444/6444
Completeness to max θ	99.9%
Absorption correction	None
Refinement method	Full-matrix least-squares on F^2
Data/restraints/parameters	6444/0/331
Goodness-of-fit on F^2	0.991
Final R indices $[I > 2\sigma(I)]$	$R_1 = 0.0622$, $wR_2 = 0.1492$
R indices (all data)	$R_1 = 0.2675$, $wR_2 = 0.2227$
Largest difference peak and hole (e Å^{-3})	0.891 and −1.710

$R_1 = \Sigma||F_o| - |F_c||/\Sigma|F_o|$; $wR_2 = (\Sigma(w(F_o^2 - F_c^2)^2)/\Sigma(w(F_o^2)^2))^{1/2}$.

of the primary beam was checked throughout the collection by monitoring three standard reflections every 60 min. On all reflections, a profile analysis was performed [20]. 2168 were observed with $I > 2\sigma(I)$. Lorentz and polarization corrections were applied. The structure was solved by Patterson methods and phase expansion using DIRDIF [21]. Empirical absorption corrections were applied at this stage using XABS2 [22]. The relative maximum and minimum transmission factors were 0.675 and 0.597, respectively. The H atoms were geometrically placed and refined riding with common isotropic thermal parameters (C–H distance = 0.93 Å). Two benzene solvent molecules, located on the mirror plane and the symmetry center, respectively, were refined with isotropic temperature factors. The molecule on the symmetry center was found highly distorted and H atoms were omitted. During the final stages of the refinement, the positional parameters and the anisotropic temperature factors for all of the non-H atoms were refined using SHELXL97 [23]. The final agreement factors are $R = 0.062$ and $wR = 0.149$, $S = 0.991$ for the 2168 'observed' reflections and 331 variables. The function minimized was $((\Sigma w F_o^2 - F_c^2)/\Sigma w(F_o^2))^{1/2}$ where $w = 1/(\sigma^2(F_o^2) + (0.0974P)^2)$ with $\sigma(F_o^2)$ from counting statistics and $P = (\text{Max}(F_o^2, o) + 2F_c^2)/3$. The maximum shift-to-error ratio in the final full matrix least-squares cycle was 0.001, while the highest and lowest peaks in the final difference Fourier calculated were 0.89 and −1.71 e Å^{-3}.

Atomic scattering factors were taken from International tables for X-ray Crystallography (1976) [24]. Plots were made with the ORTEP3 [25]. Geometrical calculations were made with PARST [26]. All crystallographic calculations were made at the Scientific Computer Centre of the University of Oviedo and on the X-ray group DEC/AXP-computers.

2.4. Computational details

All of the structures reported herein were optimized at the hybrid DFT using the Becke's three-parameter hybrid exchange-correlation functional [27] containing the nonlocal gradient correction of Lee et al. [28] (B3LYP) within the GAUSSIAN98 program [29]. All optimized structures were confirmed as minima by calculation of numerical vibrational frequencies. A collection of Cartesian coordinates and total energies for all of the optimized molecules are available from the authors upon request. Basis set for the Ru atom utilized the effective core potentials of Hay and Wadt [30] with the associated double-ζ valence basis functions. The basis set used for the remaining atomic species was the 6-311G one with the important addition of the polarization functions (d, p) for all atoms, including hydrogens.

Qualitative MO arguments, that are also very helpful in interpreting the complexity of the DFT numerical calculations, have been developed by the parallel usage of EHMO method [31] and the graphic interface to the latter provided by the package CACAO [32].

3. Results and discussion

3.1. Synthesis and spectroscopic characterization

The reaction between the dinuclear complex $(CO)_4(PPh_3)_2Ru_2[\mu\text{-}C_6H_4(NH)_2\text{-}o]$ and $CuCl_2\cdot 2H_2O$ in thf led to a brown solution. An IR spectrum of the latter showed four ν(CO) peaks at 2079, 2061, 2032 and 1996 cm^{-1}, respectively. Analogous experiments, where molecular halogen (X_2) was used in place of $CuCl_2$, also produced brown solutions which showed the same type of IR spectra with four CO peaks at 2080, 2060, 2033 and 1995 cm^{-1} (X = Br) or 2073, 2049, 2028 and 1991 cm^{-1} (X = I). Further testing in CH_2Cl_2 solution did not afford significantly different results but only slightly higher values of the ν(CO) frequencies. Accordingly,

similar compounds or mixture of them resulted from the oxidation process of the binuclear ruthenium complex. First, the characterization of the species was attempted by using chromatographic separations and fractional crystallization from the solutions. However, a better solution to the problem was found when the reactions were carried in chlorobenzene after that several other solvents had been tested. This allowed, after a few minutes, the precipitation of isolated crystalline solids (red for X = Cl, Br and brown for X = I) while the mother solution remained only slightly colored. The solids, with similar IR spectra, showed two ν(CO) peaks (Section 2) very similar to those of the solutions. Moreover, a weak intensity peak was observed at around 3100 cm^{-1} and it was assigned to ν(NH). When the residual solution, from the Br_2 reaction, was kept to crystallize after adding PPh_3 and hexane, a white solid was recovered with ν(CO) at 2065 and 1997 cm^{-1}. The IR spectrum is the same as that of the *cis* complex $[Ru(CO)_2(Br_2)(PPh_3)_2]$ that was prepared from reaction of $[Ru(CO)_3(PPh_3)_2]$ and Br_2 in CH_2Cl_2. These results confirm that the cleavage of the Ru–Ru–diimino bridge is produced by oxidants such as $CuCl_2$, Br_2 and I_2.

Further characterization of the red crystals of the bromocomplex **1** showed a *cis* arrangement of the CO ligands (two ν(CO)) and a weak ν(NH) peak. The ^{31}P NMR spectrum shows a singlet for the PPh_3 ligand. Moreover, compound **1** behaves as a 1:1 electrolyte in CH_3NO_2. All of these pieces of information, together with the results of the elemental analysis, are in agreement with the presence of a cationic species of formula $[(CO)_2(PPh_3)BrRu(diim)]^+$ and a bromide counterion. The Cl^- and I^- complexes were not equally well characterized but, on the basis of the IR spectra and of the results of the elemental analysis, analogous cations $[(CO)_2(PPh_3)XRu(diim)]^+$ can be reliably formulated.

The approximately 3100 cm^{-1} values found in all these new complexes for the ν(NH) stretching are lower than the 3325 cm^{-1} values previously found in other α-diiminobenzene complexes [9,16,33]. It may be reasonably assumed that the stronger C–N bonds (higher degree of double bonding implicit in the diimino formulation of Scheme 1) accompany to weaker N–H bonds with a less energetic vibration.

3.2. Crystal structure

The crystal structure of **1** consists of discrete monocations $[(CO)_2(PPh_3)BrRu(diim)]^+$ and bromide counterions. Also two benzene solvent molecules, arranged on symmetry elements (plane and center), are contained in the crystal lattice. An ORTEP drawing of the metal complex is presented in Fig. 1, while Table 2 reports a selection of bond distances and angles.

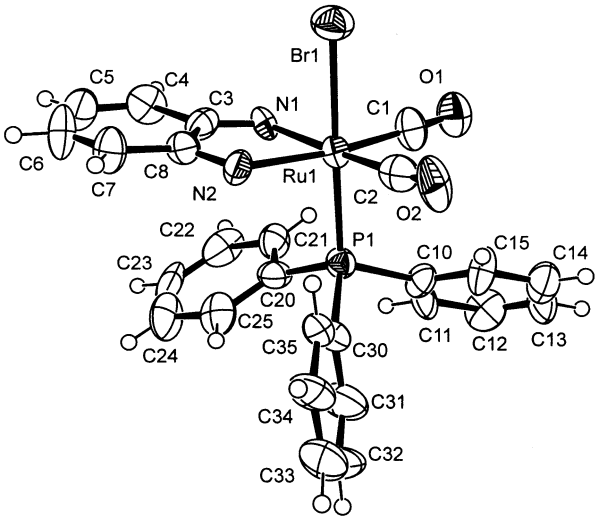

Fig. 1. An ORTEP drawing showing the structure of the complex cation $[(CO)_2(PPh_3)BrRu(diim)]^+$, **1**.

The complex cation features a ruthenium metal ion pseudo-octahedrally coordinated by *trans*-axial phosphine and bromide ligands, two *cis* carbon monoxide ligands and by a diimine chelate that completes the coordination polyhedron in the equatorial plane. The Ru–P and Ru–Br distances measure 2.336(3) and 2.560(2) Å, respectively. By comparing the latter values with those of the few structures containing the a *trans*-arrangement of the two ligands, we notice that in **1** the Ru–P distance is the longest by a few tenths of 1 Å while the Ru–Br one is the shortest (compare for instance the 2.26 and 2.65 Å found in the complex $Br(PMe_2Ph)_3(Me_2PC_6H_4)Ru$ [34]).

The Ru–N distances to the chelate of 2.07(2) and 2.08(2) Å, respectively, are >0.06 Å longer than in any other $L_4Ru(diim)$ complexes (see in particular those of [17,18]). Since **1** is the only complex featuring two carbon monoxide ligands in the equatorial plane, a considerable *trans*-influence may be likely expected in this case. Moreover, the amount of metal-chelate double bonding must be extremely limited in this complex. The point may be argumented as follows. The C–N distances of 1.26(2) and 1.29(2) Å found in **1** are the shortest ever reported for a α-diiminobenzene chelate coordinated to a single metal center (the previous record was that of the complex $(PhCN)_2(PPh_3)(H_2O)Ru(diim)$ with 1.306 and 1.296 Å, respectively [18d]). Also, the C–C bond that connects the N atoms is the longest of its type (1.51(2) Å). In addition, the inner geometry of the six-membered ring (Table 2) is highly indicative of alternating single and double bonds as it is implicit in the diimino formulation of the chelate (Scheme 1). In conclusion, even if the arrangement of the chelate in the equatorial plane is suited for a π type interaction with the metal atom (backdonation), this must particularly weak in view the long Ru–N distances. In other words,

Table 2
A selection of bond lengths [Å] and angles [°] for the complex cation $[(CO)_2(PPh_3)BrRu(C_6H_4(NH)_2\text{-}o)]^+$ present in the crystal structure of **1**

Bond distances	
Ru(1)–P(1)	2.336(3)
Ru(1)–Br(1)	2.560(2)
Ru(1)–C(1)	1.89(2)
Ru(1)–C(2)	1.97(2)
Ru(1)–N(1)	2.07(1)
Ru(1)–N(2)	2.08(1)
P(1)–C(20)	1.80(1)
P(1)–C(30)	1.81(1)
P(1)–C(10)	1.82(1)
O(1)–C(1)	1.13(2)
O(2)–C(2)	1.08(2)
N(2)–C(8)	1.29(2)
N(1)–C(3)	1.26(2)
C(3)–C(4)	1.45(2)
C(4)–C(5)	1.37(2)
C(5)–C(6)	1.44(2)
C(6)–C(7)	1.31(2)
C(7)–C(8)	1.41(2)
C(3)–C(8)	1.51(2)
C–C (phenyl 10–15, ave.)	1.38(3)
C–C (phenyl 20–25, ave.)	1.37(2)
C–C (phenyl 30–35, ave.)	1.38(2)
Bond angles	
P(1)–Ru(1)–Br(1)	178.8(1)
C(1)–Ru(1)–Br(1)	88.9(5)
C(2)–Ru(1)–Br(1)	87.1(4)
N(1)–Ru(1)–Br(1)	87.2(3)
N(2)–Ru(1)–Br(1)	87.9(3)
C(1)–Ru(1)–P(1)	89.9(5)
C(2)–Ru(1)–P(1)	92.4(4)
N(1)–Ru(1)–P(1)	93.4(3)
N(2)–Ru(1)–P(1)	93.3(3)
C(1)–Ru(1)–C(2)	92.3(6)
N(1)–Ru(1)–N(2)	76.8(4)
C(1)–Ru(1)–N(1)	93.9(5)
C(2)–Ru(1)–N(1)	171.6(5)
C(1)–Ru(1)–N(2)	170.3(5)
C(2)–Ru(1)–N(2)	96.7(5)
O(1)–C(1)–Ru(1)	178(1)
O(2)–C(2)–Ru(1)	177(1)
C(20)–P(1)–C(30)	105.0(6)
C(20)–P(1)–C(10)	108.1(6)
C(30)–P(1)–C(10)	101.8(6)
C(10)–P(1)–Ru(1)	113.0(4)
C(20)–P(1)–Ru(1)	110.4(4)
C(30)–P(1)–Ru(1)	117.7(5)
C(8)–N(2)–Ru(1)	116.2(8)
C(3)–N(1)–Ru(1)	116.6(8)
N(1)–C(3)–C(4)	127(1)
N(1)–C(3)–C(8)	116(1)
C(4)–C(3)–C(8)	117(1)
N(2)–C(8)–C(7)	126(1)
N(2)–C(8)–C(3)	114(1)
C(7)–C(8)–C(3)	120(1)
C(5)–C(4)–C(3)	119(1)
C(6)–C(7)–C(8)	120(1)
C(4)–C(5)–C(6)	121(1)
C(7)–C(6)–C(5)	123(1)

there is enough structural evidence that the electronic perturbation of the metal over the π system of the diimino ligand is minimum.

3.3. Electrochemistry

The cyclic voltammetry experiments, carried out in dichloromethane at room temperature, show an reduction peak at −0.2 V (in an one-electron process). This accounts for the easy formation of the neutral species $[(CO)_2(PPh_3)BrRu(diim)]$ where the chelate ligand has acquired the presumable semiquinone character. The further one electron oxidation that restores to the original monocation is inferred from the low intensity oxidation peak at −0.08 V and by the quasi reversibility of the process at the given scan rate of 50 mV s^{-1} with a peak current ratio $I_{p.a}/I_{p.c} = 1.4$. The Fc/Fc^+ redox couple was used as an internal standard. In this case, the fast addition and removal of one electron from the primary pseudo-octahedral complex is well tolerated and it does not seem to induce any major structural change. This situation is substantially similar to that already reported for the complex $(SnPh_3)_2(CO)_2Ru(iPr\text{-}DAB)$ [5] where, however, a full electrochemical reversibility is indicated by the peak current ratio $I_{p.a}/I_{p.c}$ of 1. However, when the scan rate is lowered to 10 mV s^{-1}, the reduction peak is still clearly showed (at −0.18 V) but the corresponding oxidation peak is almost disappeared. This may be taken as a proof of a relatively low stability of the neutral hexa-coordinated species that is evidentiated in the longer run. The redox process and the stability of the relative species will be later considered from the theoretical viewpoint.

4. Theoretical analysis

4.1. General considerations

In order to provide an overview of the electronic features of the pseudo-octahedral ruthenium(II) complexes of the type $L_4Ru(diim)$, it is useful to consider the interaction diagram of Fig. 2.

At the left side, the typical frontier orbitals of the C_{2v} butterfly fragment are shown [35]. These consist of a low lying set of t_{2g} orbitals and two higher $\pi_{\|}$ and σ hybrids. The latter are suited to accept the donation of two symmetry adapted combinations of nitrogen lone pairs at the chelate (lower levels at the right side of Fig. 2). At the left side, the t_{2g} orbitals must be considered all populated (see in Scheme 3 their distinctive d_σ, d_δ and d_π characters), in agreement with a d^6 configuration for Ru(II). Their energy is lower than that of the critical π* level of the chelate. Being the latter empty, the chelate must be formulated as α-diimino. In contrast, the diamido formulation applies best to the Group 6

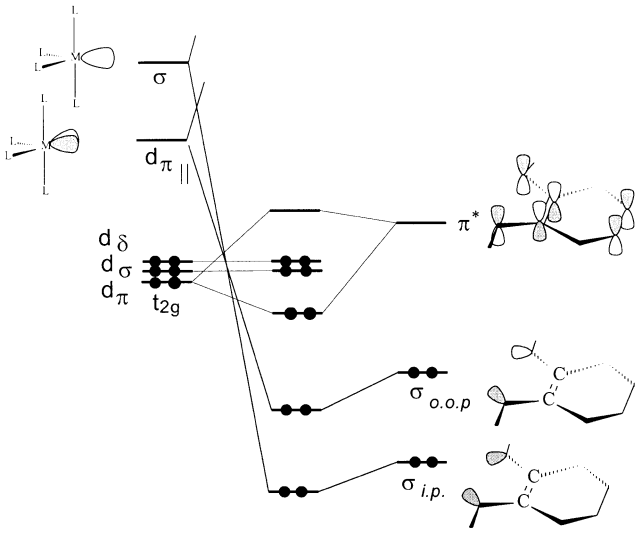

Fig. 2. General diagram for the interaction between a butterfly fragment d^6-L_4M (M = Group 8 metal) and a α-diimino chelate lying in the equatorial plane.

isoelectronic Mo(II) complexes [6]. For the latter, the relative order of t_{2g} and π* levels is inverted as it can be simply verified from the table of H_{ii} parameters used in EHMO calculations [36]. According to the latter, the d orbitals of ruthenium are approximately 1.8 eV lower in energy than those of molybdenum.

The inverted energy order with respect to the ligand's π* level is fundamental in determining electronic and structural differences between L_4M(*diim*) complexes of the two groups of metals [6]. In the isoelectronic complex $(CO)_2(PPh_3)_2Mo[C_6H_4(NH)_2$-*o*$]$ [9], the π* MO should be considered filled, hence it can donate a third electron pair into the empty d_π–t_{2g} orbital (Scheme 3). In actuality, the latter can be assigned to the category of octahedral d^4 complexes that are Jahn–Teller unstable [10] and whose distortional trends have been the subject of a previous detailed study [37]. Concerning the above Mo(II) complex, the evident effect is the rotation of the chelate about its C_2 axis and out of the equatorial plane [9]. The latter is well reproduced computationally [6].

In the isoelectronic ruthenium hexa-coordinated species, the π* MO lies higher than the t_{2g} levels and the regular octahedral geometry, expected for d^6 metals, is observed (C_{2v} symmetry). Importantly, these complexes may be electronically reduced on account of the relatively low lying LUMO. Given the nature of the latter, the added electrons are hosted by the chelate rather than by the metal itself. In fact, the composition of the LUMO is significantly different with respect to the Group 6 analogues. For example, the LUMO of the model $(CO)_2(PPh_3)_2Mo[C_6H_4(NH)_2$-*o*$]$ features $>50\%$ metal character whereas the percentage drops to $<20\%$ for the isoelectronic ruthenium model. The addition of two electrons transforms the bonding d_π/π^* interaction into a destabilizing four electrons repulsion and seems sufficiently well tolerated by the Group 6 metals that complete in this manner the population of the t_{2g} shell. An indication is provided by the calculations on the dianionic complexes of the type $[(CO)_4W(C_6H_4(NR)_2)]^{-2}$ [6]. Dissociation of the latter complex (experimentally unknown) into a stable 18 electron five coordinated complex and a free carbonyl ligand is computed to be endothermic. Also, it has been mentioned in the introduction that the presence of *o*-phenylenedisulfide or *o*-phenylenediphosphido chelates allows to isolate experimentally the dianionic octahedral complexes of tungsten [14].

No two electrons reduced derivative has been ever structurally characterized for Ru(II) hexa-coordinated complexes. Conversely, the addition of a single electron seems to be tolerated without disruption of the primary pseudo-octahedral geometry. This is confirmed by the quasi reversibility of the cyclovoltammogram of **1** in the fast scan rate. It is worth mentioning, in this respect, the very accurate experimental and theoretical studies reported by other authors for systems of the type $(CO)_2LL'Ru$(iPr-DAB) ($L' = SnR_3$, CH_3, Cl) [38], where the chelate is a most simple α-diimino molecule with no aromatic backbone. In this case, the reduction to the monoanion is fully reversible with the added electron populating a π* level of the ligand (the SOMO has again mixed C–C π and C–N π* characters). The calculations, performed for the ground and the excited states, well justify the unusual visible and EPR spectra, a distinguished role being played by the axial SnR_3 ligand(s), when present.

4.2. Detailed computational results

We first present in Fig. 3 the optimized structure of complex **1**, where a PH_3 replaces the triphenylphosphine ligand. The agreement with the experimental structure can be considered satisfactory. The structure maintains

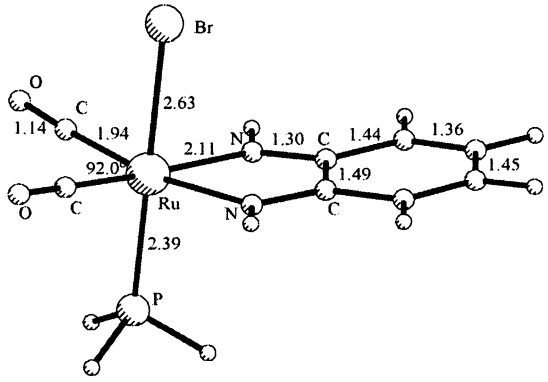

Fig. 3. Optimized structure of complex cation $[(CO)_2(PH_3)Br$-$Ru(C_6H_4(NH)_2$-*o*$)]^+$, a model of the experimentally determined compound **1**.

a fairly regular pseudo-octahedral geometry with the chelate in the equatorial plane (C_s symmetry). The computation shows only slight elongations (0.05–0.07 Å) of the Ru–Br and Ru–P axial bonds with respect to the experiment. Also the Ru–N bonds are somewhat longer than in the experiment (2.110 vs 2.075 Å, ave.). The geometry of the chelate is fully consistent with the diimino formulation (Scheme 1) with alternating single and double bonds within the planar chelate.

Next, we have optimized the structure of the dication $[(PH_3)_4Ru(diim)]^{2+}$, **2a**. This model has been selected because, upon a two electrons reduction and the loss of one phosphine ligand, is potentially transformed into complex $[(PH_3)_3Ru(diim)]$, **3a**, that is most similar to the experimentally known complex $(PPh_3)_3Ru[C_6H_4(NH)_2$-*o*], **3** [16]. We have systematically followed the transformations of **2a** on reduction, by optimizing the structure of the radical monocation, **2b**, and that of the uncharged pseudo-octahedral derivative **2c**. All of the latter structures, that appear to be stationary points, are reported in Fig. 4. Finally, we have also performed the optimization of the five coordinated species **3a** that may be derived from **2c** upon the loss of one phosphine ligand (vide infra).

The geometry of the dication **2a** is consistent with that of bromide complex of Fig. 1. Although the monocation **2b** does not present unusual strains, there is a clear cut indication that the added electron is localized on the chelate (similarly to the analogous situation reported for the complex with ligand iPr-DAB [34]). In fact, there is simultaneous lengthening of the C–N distances (from 1.31 to 1.35 Å) and shortening of the C–C one (from 1.49 to 1.45 Å). No evident variation of distances takes place inside the $(PH_3)_4Ru$ fragment and also the Ru–N bonds seem unaffected (2.11 Å, in both **2a** and **2b**), whereas the angle P_{ax}–Ru–P_{ax} closes up about 10°. All

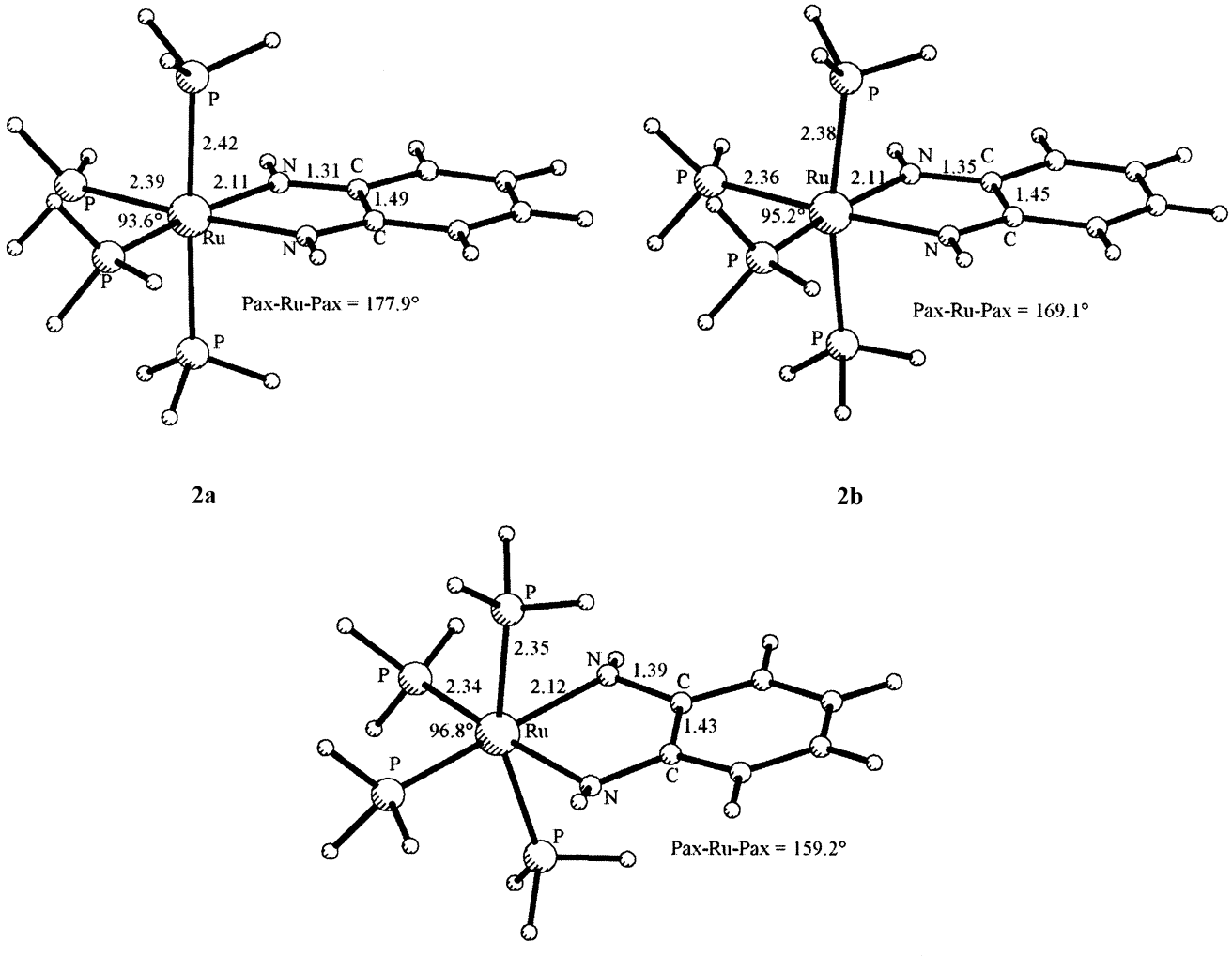

Fig. 4. Optimized structures of the complexes $[(PH_3)_4Ru(C_6H_4(NH)_2$-*o*$)]^{2+,\,1+,\,0}$ (**2a**, **2b** and **2c**, respectively). For the sake of consistency, all the structures were optimized with C_2 symmetry.

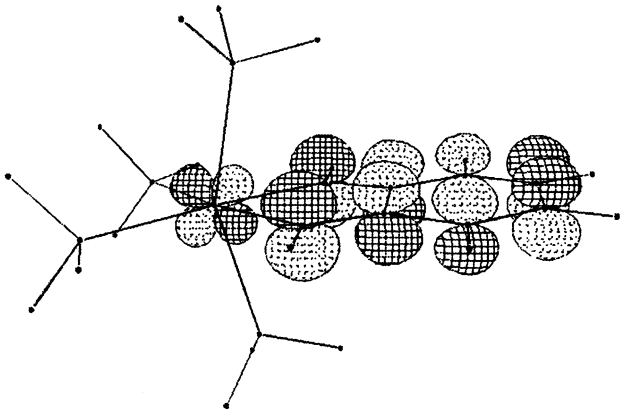

Scheme 4.

of the latter effects are further magnified in the most reduced complex **2c**. Not only the C–C and the C–N distances attain their smallest and largest values of 1.43 and 1.39 Å, respectively, but also the angle P_{ax}–Ru–P_{ax} is closed by another 10°. A qualitative explanation for the latter effects may be quickly gained by constructing a Walsh diagram at the simplest EHMO level. The HOMO, with anti-bonding character between the metal d_π and ligand π* MO (hence the significant four electrons repulsion) stabilizes on bending the axial phoshine ligands toward the chelate. The CACAO drawing of the HOMO (Scheme 4) shows that the lobes of the d_π metal orbital rehybridizes on the side opposite to the ligand's π lobes. This helps to reduce somewhat and the four-electron repulsion.

The optimization of **2c** also shows an evident strain at the chelate itself. In fact, while the C_6 ring remains planar, the N atoms are off of the plane (NCCN dihedral angle of 14°). Moreover, each N donors is evidently pyramidalized, with the attached H atom pinning up or down the ligand's plane.

In actuality, there is no experimental evidence that **2c** can be an electronically stable complex. Although the optimized species is a stationary point (zero imaginary frequencies), energetic evaluations suggest that the dissociation of one PH_3 ligand is favored. In fact, upon the optimization of **3** (vide infra) we find that the process $\mathbf{2c} \rightarrow \mathbf{3} + PH_3$ is exothermic by about 3.7 kcal mol^{-1}. At this point, it is worth noticing that the analogous dissociation of one carbonyl ligand from the complex $[(CO)_4Mo(C_6H_4(NR)_2)]^{-2}$ was calculated to be an endothermic process of about 17 kcal mol^{-1} [6,14]. This confirms a significantly different nature of the bonding in $L_4M(diim)$ complexes of Group 6 and Group 8 metals.

Two different structural optimizations have been carried out for **3**, namely that of a trigonal bipyramidal model with imposed C_s symmetry (**3a**) and that of a square pyramid (**3b**), that is also very close to C_s symmetry, although no constrain was imposed (C_1). Both models are reported in Fig. 5. The geometric parameters are very similar in the two cases, except for the simultaneous elongation and shortening of the Ru–N apical and equatorial bonds in **3a** (the 2.03 equivalent values in **3b** become 2.06 and 2.01 Å, respectively). One imaginary frequency of mode A″ is computed for **3a**,

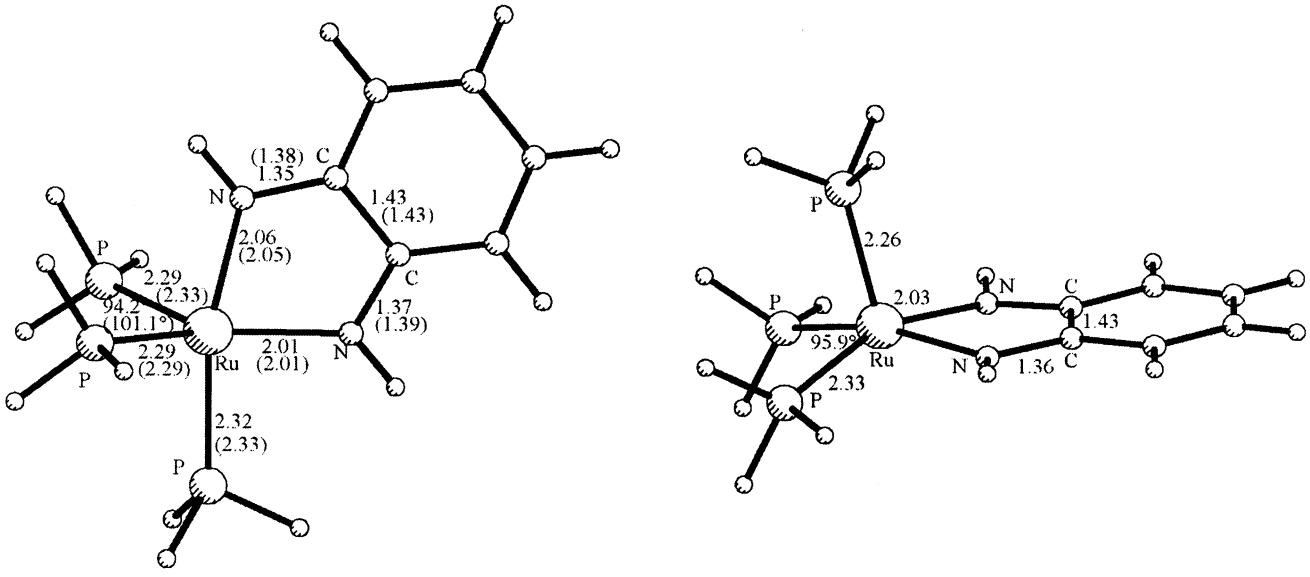

3a **3b**

Fig. 5. Optimized trigonal bipyramidal (**3a**) and square pyramidal (**3b**) model of the complex $(PPh_3)_3Ru[C_6H_4(NH)_2$-*o*$]$, **3**. The parenthetical values, present in the drawing of **3**a, are those of the experimental structure of [16].

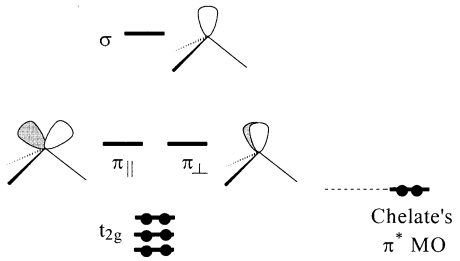

Scheme 5.

thus suggesting that the chelate does not want to lie in the symmetry plane. Since the NMR spectra of **3** are indicative of fluxionality of the chelate with respect to the P_3Ru unit [16], the structure **3a** may be taken as the transition state for the reciprocal rearrangements of the threefold rotor (L_3M fragment) with respect to the twofold one (the chelate itself). The barrier for such a rearrangement is computed to be only 1.1 kcal mol^{-1} ($E_{3b}-E_{3a}$). Notice that, in the crystal structure, the complex of $(PPh_3)_3Ru[C_6H_4(NH)_2$-*o*$]$ [16] is significantly closer to the TBP geometry, the chelate being only 12° skewed from the orthogonality with a P_2Ru plane.

At variance with the stable hexa-coordinated precursor **2a** (and the model of **1** as well), the chelate ligand in **3a** and **3b** is more consistent with the diamido formulation. The computed C–N and C–C bonds, that in **2a** measured 1.31 and 1.49 Å, are now 1.36 (average) and 1.43 Å, respectively. This is a clear indication that the diimino/diamido dichotomy is not exclusively governed by the nature of the metal but also by its environment. The hybridization and energies of the metal frontier orbitals that may interact with the chelate are substantially different in L_3M and L_4M fragments. The removal of one ligand from the latter leaves unsaturated a high lying σ orbital of the metal. The energy of the latter is lowered upon the rearrangement of the fragment a trigonal pyramid but it is still relatively high. In fact, the frontier orbital region is that classically described [35] and reported in Scheme 5. Irrespective from the orientation of the chelate, either in the plane (TBP) or upright (SP), the higher σ hybrid and one of the lower d_π hybrids get involved in σ bonding with the two combinations of σ lone pairs at the chelate. The other degenerate d_π level is suited to interact with the ligand's π* MO (Scheme 2). At variance with the situation of Fig. 1, the chelate's orbital lies lower than its d_π metal partner and it's the best candidate to host the electron pair of their bonding interaction (diamido formulation).

5. Conclusions

In this paper, we have presented a new complex of the type L_4Ru(*diim*) that has given us the impulse to revise the structural and electronic features of the few known monomeric complexes of Group 8 metals containing an α-diiminobenzene chelate (*diim*, $C_6H_4(NR)_2$-*o*). At variance with analogous pseudo-octahedral complexes of Group 6 metals, the diimino formulation for this ligand is the most chemically intuitive as confirmed by the trends for the structural parameters. This is also corroborated by the DFT calculations and their interpretation in terms qualitative MO theory. However, it cannot be concluded that the diimino/diamido dichotomy is governed by the nature of the metal alone. In fact, the coordination to a L_3Ru(II) fragment restores the capability of the ligand to chelate the metal in its most reduced dianionic form. The origin of the dichotomy in these compounds can be traced back by using simple perturbation theory arguments and by considering the significantly different hybridization and energies of L_4M and L_3M fragments. A resume of the different situation encountered in the analogous complexes of Group 6 metals [6] has been also provided for convenience.

6. Supplementary material

The structural results (excluding structure factors) have been deposited at the Cambridge Crystallographic Data Center, CCDC No. 194391. Copies of the data can be obtained free of charge on application to The Director, CCDC, 12 Union Road, Cambridge CB2 1EZ, UK (fax: +44-1223-336-033, e-mail: teched @ccdc.cam.ac.uk or www: http://www.ccdc.cam.ac.uk).

Acknowledgements

Thanks are expressed to CICYT (BQU2000-0227) and the Principado de Asturias (PR-01-GE-6) (R.O.-R.), CICYTC (BRU2000-0219), FICYT (PR-01-GE-4) and DGESIC (A.G.) for support. Part of the work has been carried out during a visit of C. M. at the University of Sevilla financed by the Junta de Andalucía. A.G. acknowledges the financial support provided by the Secretaria de Estado de Universidades e Investigación for a sabbatical stage at ICCOM.

References

[1] (a) L.H. Gade, Chem. Commun. (2000) 173;
(b) T.M. Cameron, I. Ghiviriga, K.A. Abboud, J.M. Boncella, Organometallics 20 (2001) 4378;
(c) R.C. Mills, K.A. Abboud, J.M. Boncella, Chem. Commun. (2001) 1506;
(d) T.M. Cameron, K.A. Abboud, J.M. Boncella, Chem. Commun. (2001) 1224;
(e) T.M. Cameron, C.G. Ortiz, I. Ghiviriga, K.A. Abboud, J.M. Boncella, Organometallics 20 (2001) 2032.

[2] H.-L. Chan, H.-Q. Liu, B.-C. Tzeng, Y.-S. You, S.-M. Peng, M. Yang, C.-M. Che, Inorg. Chem. 41 (2002) 3161.
[3] C. Mealli, A. Ienco, A. Anillo, S. Garcia-Granda, R. Obeso-Rosete, Inorg. Chem. 36 (1997) 3724.
[4] (a) O. Carugo, K. Djinovic, M. Rizzi, C.B. Castellani, J. Chem. Soc. Dalton Trans. (1991) 1551;
(b) S.J.N. Burgmayer, H.L. Kaufmann, G. Fortunato, P. Hug, B. Fischer, Inorg. Chem. 38 (1999) 2607;
(c) J. Van Slageren, A. Klein, S. Záliš, D.J. Stufkens, Coord. Chem. Rev. 219–221 (2001) 937;
(d) H. Masui, A.B.P. Lever, P.R. Auburn, Inorg. Chem. 30 (1991) 2402.
[5] M.P. Aarnts, M.P. Wils, K. Peelen, J. Fraanje, K. Goubitz, F. Hartl, D.J. Stufkens, E.J. Baerends, A. Vlček, Jr., Inorg. Chem. 35 (1996) 5468 (and references therein).
[6] A. Galindo, A. Ienco, C. Mealli, Comments Inorg. Chem. 23 (2002) 401.
[7] J.M. Boncella, S.-Y.S. Wang, D.D. VanderLende, R.L. Huff, K.A. Abboud, W.M. Vaughn, J. Organomet. Chem. 530 (1997) 59.
[8] (a) A. Galindo, A. Ienco, C. Mealli, New J. Chem. 24 (2000) 73;
(b) A. Galindo, M. Gómez, D. del Río, F. Sánchez, Eur. J. Inorg. Chem. (2002) 1326;
(c) D. del Río, A. Galindo, J. Organomet. Chem. 655 (2002) 16.
[9] A. Anillo, R. Obeso-Rosete, M. Lanfranchi, A. Tiripicchio, J. Organomet. Chem. 453 (1993) 71.
[10] H.A. Jahn, E. Teller, Phys. Rev. 49 (1936) 874.
[11] R.C. Mills, S.-Y.S. Wang, K.A. Abboud, J.M. Boncella, Inorg. Chem. 40 (2001) 5077.
[12] W.H. Leung, A.A. Danopoulos, G. Wilkinson, B. Hussain-Batea, M.B. Hursthouse, J. Chem. Soc. Dalton Trans. (1991) 2051.
[13] D.J. Darensbourg, K.K. Klausmeyer, J.H. Reibenspies, Inorg. Chem. 35 (1996) 1535.
[14] D.J. Darensbourg, J.D. Draper, B.J. Frost, J.H. Reibenspies, Inorg. Chem. 38 (1999) 4705.
[15] (a) F.H. Allen, O. Kennard, Chem. Des. Autom. News 8 (1993) 31;
(b) CSD version 5.23 (April 2002).
[16] A. Anillo, C. Barrio, S. Garcia-Granda, R. Obeso-Rosete, J. Chem. Soc. Dalton Trans. (1993) 1125.
[17] G.G. Christoph, V.L. Goedken, J. Am. Chem. Soc. 95 (1953) 3869.
[18] (a) D. Venegas-Yazigi, H. Mirza, A.B.P. Lever, A.J. Lough, J. Costamagna, A. Vega, R. Latorre, Acta Crystallogr., C 56 (2000) e245;
(b) D. Venegas-Yazigi, H. Mirza, A.B.P. Lever, A.J. Lough, J. Costamagna, A. Vega, R. Latorre, Acta Crystallogr., C 56 (2000) e247;
(c) D. Venegas-Yazigi, H. Mirza, A.B.P. Lever, A.J. Lough, J. Costamagna, A. Vega, R. Latorre, Acta Crystallogr., C 56 (2000) e281;
(d) D. Venegas-Yazigi, H. Mirza, A.B.P. Lever, A.J. Lough, J. Costamagna, A. Vega, R. Latorre, Acta Crystallogr., C 56 (2000) e323.
[19] S. García-Granda, R. Obeso-Rosete, J.M. Rubio, A. Anillo, Acta Crystallogr., C 46 (1990) 2043.
[20] (a) D.F. Grant, E.J. Gabe, J. Appl. Cryst. 11 (1978) 114;
(b) M.S. Lehman, F.K. Larsen, Acta Crystallogr., A 30 (1974) 580.
[21] P.T. Beurskens, G. Beurskens, W.P. Bosman, R. de Gelder, S. Garcia-Granda, R.O. Gould, R. Israel, J.M.M. Smits. The DIRDIF96 Program System, Technical Report of the Crystallography Laboratory, University of Nijmegen, Nijmegen, The Netherlands, 1996.
[22] S. Parkin, B. Moezzi, H. Hope, J. Appl. Cryst. 28 (1995) 53.
[23] G.M. Sheldrick, SHELXL-97. Program for the Refinement of Crystal Structures, University of Göttingen, Göttingen, Germany, 1997.
[24] International Tables for X-ray Crystallography, Vol. IV, Birmingham, Kynoch Press. (Present distributor: Kluwer Academic Publishers, Dordrecht), 1974.
[25] L.J. Farrugia, ORTEP3 for Windows, J. Appl. Cryst. 30 (1997) 565.
[26] M. Nardelli, Comput. Chem. 7 (1983) 95.
[27] A.D. Becke, J. Chem. Phys. 98 (1993) 5648.
[28] C. Lee, W. Yang, R. Parr, G. Phys. Rev. B 37 (1988) 785.
[29] Gaussian 98, Revision A.7:, M.J. Frisch, G.W. Trucks, H.B. Schlegel, G.E.M. Scuseria, A. Robb, J.R. Cheeseman, V.G. Zakrzewski, J.A. Montgomery, R.E. Stratmann, J.C. Burant, S. Dapprich,; J.M. Millam, A.D. Daniels, K.N. Kudin, M.C. Strain, O. Farkas, J. Tomasi, V. Barone, M. Cossi, R. Cammi, B. Mennucci, C. Pomelli, C. Adamo, S. Clifford, J. Ochterski, G.A. Petersson, P.Y. Ayala, Q. Cui, K. Morokuma, D.K. Malick, A.D. Rabuck, K. Raghavachari, J.B. Foresman, J. Cioslowski, J.V. Ortiz, B.B. Stefanov, G. Liu, A. Liashenko, P. Piskorz, I. Komaromi, R. Gomperts, R.L. Martin, D.J. Fox, T. Keith, M.A. Al-Laham, C.Y. Peng, A. Nanayakkara, C. Gonzalez, M. Challacombe, P.M.W. Gill, B.G. Johnson, W. Chen, M.W. Wong, J.L. Andres, M. Head-Gordon, E.S. Replogle, J.A. Pople, Gaussian, Inc., Pittsburgh, PA, 1998.
[30] P.J. Hay, W.R. Wadt, J. Chem. Phys. 82 (1985) 299.
[31] (a) R. Hoffmann, W.N. Lipscomb, J. Chem. Phys. 36 (1962) 2872;
(b) R. Hoffmann, W.N. Lipscomb, J. Chem. Phys. 37 (1962) 3489.
[32] (a) C. Mealli, D.M. Proserpio, J. Chem. Educ. 67 (1990) 399;
(b) C. Mealli, A. Ienco, D.M. Proserpio, Book of Abstracts of the XXXIII ICCC, Florence, 1998, p. 510.
[33] (a) A. Anillo, R. Obeso-Rosete, M.A. Pellinghelli, A. Tiripicchio, J. Chem. Soc. Dalton Trans. (1991) 2019;
(b) A. Anillo, S. García-Granda, R. Obeso-Rosete, J.M. Rubio, J. Chem. Soc. Dalton Trans. (1993) 3287.
[34] S.D. Chappell, L.M. Engelhardt, A.H. White, C.L. Raston, J. Organomet. Chem. 462 (1993) 295.
[35] A. Albright, J.K. Burdett, M.H. Whangbo, Orbital Interactions in Chemistry, Wiley, New York, 1985.
[36] S. Alvarez, Tables of Parameters for Extended Hückel Calculations, Departamento de Quimica Inorgánica, Universidad de Barcelona, Barcelona, Spain, 1989.
[37] P. Kubáček, R. Hoffmann, J. Am. Chem. Soc. 103 (1981) 4320.
[38] M. Turki, D. Chantal, S. Zális, A. Vlček, J. van Slageren, D.J. Stufkens, J. Am. Chem. Soc. 123 (2001) 11431.